BILINGUAL PUBLISHING GROUP

Journal of Environmental & Earth Sciences

https://journals.bilpubgroup.com/index.php/jees

ARTICLE

Uranium Species in Peat and Rock Sediments Near Sludge Storage Facility

Olga Shvartseva [1,2*] **, *Daria Mashkova*** [2]

[1] *X-BIO Institute of Environmental and Agricultural Biology, University of Tyumen, 625003 Tyumen, Russia*

[2] *V.S. Sobolev Institute of Geology and Mineralogy Siberian Branch Russian Academy of Science, 630090 Novosibirsk, Russia*

ABSTRACT

The study aims to investigate uranium species in the sediments of the natural-technogenic system within a sludge storage facility in Russia. The relevance of this work is underscored by the need to assess the geochemical mobility of radionuclides, a critical factor for predicting their migration and environmental impact. The objective of the research was to determine the uranium species in both peat and sedimentary rock samples of the sludge storage facility and the adjacent area. Laboratory analyses included XRD, XRF analysis using synchrotron radiation, and scanning electron microscopy to study the composition and properties of minerals. The uranium species were further identified using a modified Tessier sequential extraction method. The results revealed that uranium predominantly occurs in a stable silicate-bound form (up to 80%) in sedimentary rocks, indicating minimal geochemical mobility. In contrast, in peat deposits, uranium is primarily associated with manganese and iron oxides (30–60%) as well as organic matter (5–40%), with the most mobile forms constituting less than 5%. The decrease in uranium concentration with distance from the facility was attributed to sorption onto organic matter and co-precipitation with mineral compounds, manganese and iron oxides, which serve as effective natural sorbents. The findings highlight the critical role of organic matter and metal oxides in limiting uranium migration, thus identifying them as key components in the formation of natural barriers for radionuclides. These results are crucial for assessing environmental risks associated with radioactive waste management and for developing strategies to minimize the

*CORRESPONDING AUTHOR:

Olga Shvartseva, X-BIO Institute of Environmental and Agricultural Biology, University of Tyumen, 625003 Tyumen, Russia; V.S. Sobolev Institute of Geology and Mineralogy Siberian Branch Russian Academy of Science, 630090 Novosibirsk, Russia; Email: o.s.shvarceva@utmn.ru

ARTICLE INFO

Received: 20 November 2024 | Revised: 4 December 2024 | Accepted: 6 December 2024 | Published Online: 7 February 2025
DOI: https://doi.org/10.30564/jees.v7i2.7831

CITATION

Shvartseva, O., Mashkova, D., 2025. Uranium Species in Peat and Rock Sediments Near Sludge Storage Facility. Journal of Environmental & Earth Sciences. 7(2): 187–197. DOI: https://doi.org/10.30564/jees.v7i2.7831

ecological impact of sludge storages.

Keywords: Uranium; Sludge Storage; Mineral Composition; Uranium Speciation in Sediments; Sorption by Peat; XRD; SEM; Safe Management

1. Introduction

Radioactive waste storage facilities created by enterprises involved in the nuclear fuel cycle represent a distinct class of geochemical anomalies [1]. The chemical forms in which radionuclides can be released into the environment are highly diverse and depend on the technological processes employed during their synthesis [2]. Developing a scientifically substantiated forecast regarding changes in radionuclide properties during their migration and redistribution requires understanding and accounting for the specific local conditions governing their interaction with the environment [2–6]. Notably, the forms in which radionuclides occur determine their geochemical mobility, transport rate, biological hazard, and potential impact on humans [4–8].

The physicochemical mechanisms governing the transport of anthropogenic radionuclides remain insufficiently studied, primarily due to methodological challenges and the inherent complexity of identifying radionuclide forms in aquatic systems, given their ultra-low concentrations [9–11]. Scientific interest in determining elemental forms has grown steadily since the late 20th century. Foundational studies have emphasized the necessity of examining the forms of radionuclide occurrence [12–16]. A primary focus of such research is to identify the forms of occurrence of heavy metals, radionuclides, and major cations to elucidate the factors driving the formation of stable geochemical bonds, depending on the hydrogeological and biogeochemical parameters of the environment [7, 11–13, 17–30]. Studies also explore the migration patterns and forms of occurrence of metals, spatial variations in the transport of strongly sorbent compounds [31], and the distribution of elements among suspended, dissolved, and precipitated fractions [5, 32–34].

Uranium contamination is of particular importance, as uranium is classified as a long-lived radionuclide with significant environmental and biological risks. Its geochemical behavior depends primarily on its oxidation state, with hexavalent uranium being highly mobile and tetravalent uranium tending to form stable precipitates [9, 30, 35, 36]. The mobility of uranium is further influenced by environmental factors such as pH, redox potential, organic matter, and the presence of metal oxides, which act as either sorbents or co-precipitants [30, 37]. These factors are critical for defining the environmental fate of uranium, particularly in natural-technogenic systems impacted by radioactive waste storage facilities. Understanding the mechanisms behind uranium transport and immobilization is essential for mitigating its environmental impact and ensuring the safety of ecosystems and human health [37].

The geochemical mobility, migration rate, sedimentation dynamics, and biological hazard of toxic elements in water are determined by their forms of occurrence, which, in turn, are influenced by key environmental parameters: pH, redox potential, salinity, and the chemical type of solutions, as well as the total organic matter content. Questions concerning the quantitative changes in aggregated states under in situ-controlled parameters remain highly debated [30, 31, 35, 36].

The sources of radionuclides, along with the mechanisms of their migration and deposition, play a central role in defining their forms of occurrence in the environment [37, 38]. The intensity of anthropogenic radionuclide migration and their impact on ecosystems and living organisms are pressing scientific and practical issues [39, 40]. A detailed investigation of the forms of occurrence of macronutrients, alongside radionuclides, is essential for understanding the mechanisms of substance transport in aquatic systems. Such studies reveal the key factors that govern radionuclide behavior, which are necessary for developing migration models and long-term forecasts of their behavior within a system.

The aim of this study is to determine the forms of uranium occurrence in the underlying sediments of the natural-technogenic system of the tailings storage facility at the Novosibirsk Chemical Concentrates Plant (NCCP) and the surrounding area. Specifically, the study focuses on identifying the predominant forms of uranium, assessing their environmental mobility, and understanding the mechanisms that influence its distribution. These findings will contribute to developing more accurate models of radionuclide migration

and inform strategies for improving environmental safety at radioactive waste storage facilities.

2. Materials and Methods

2.1. Object of Study

The object of this study is the low-level radioactive waste (LLRW) tailings storage facility of NCCP and the adjacent area affected by the enterprise's operations (**Figure 1**). The area designated for waste storage covers approximately 120 hectares. The tailings repository consists of two sections: one that has been decommissioned and mothballed, and another that has been operational since 1964.

The repository serves as a long-term storage facility for LLRW. The basin of the operational section is enclosed by a permeable dam constructed from local soils containing uranium ore tailings. Slurry containing liquid LLRW is transported via pipeline to the repository dump. Until the mid-20th century, the enterprise processed ores for uranium mineral extraction. Currently, however, the plant produces uranium dioxide powder without ore processing. This technological shift has altered the composition of the waste; modern waste is devoid of uranium decay products, accounting for the absence of gamma activity in these deposits [41].

The following liquid waste disposal scheme is used at the facility: acidic highly mineralized solutions are neutralized with lime slurry (a solution of $Ca(OH)_2$), followed by the discharge of neutralized solutions into the dump. Suspended particles precipitate, and a portion of the neutralized solutions mix with groundwater, infiltrating the underlying deposits through the bottom and walls of the sludge repository. In the process of the acidic tails' neutralization, the solution quickly becomes supersaturated with respect to calcite, gypsum, dolomite, and barite. If the initial solutions contain high concentrations of fluoride ion, then during neutralization there is an active formation of fluorite (CaF_2), which in some cases can form the bulk of the waste [42]. Water seeps not only through the bottom and walls of the sludge repository, but also filters through the dam, leaving the surface flow of the stream towards the river [43]. Apart from acid anions, water can have an increased content of uranium and heavy metals. The content of uranium in waters is influenced by their redox potential; under the reducing conditions, uranium changes to a four-valent form and precipitates from solutions. The nitrate ion, acting as a strong oxidizer, **raises the redox potential (Eh)** in waters to +300–+400 mV; uranium is therefore in hexavalent form, which prevents its precipitation on clays and organics [41].

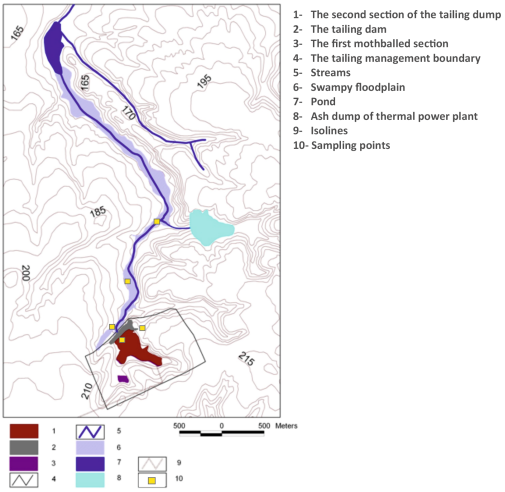

Figure 1. Sampling scheme at the sludge storage site.

Host rocks at the site are represented by middle Quaternary fluviolacustrine sediments and can be divided into three layers. A 3–9 m thick layer of loam is located at the bottom. The overlying layer is composed of intercalations of yellowish-brown loam with sandy loam and fine-grained sand. The layer at the top consists of loess-like yellowish-brown loam with a thickness of 8–15 m. Along the stream, a swampy floodplain has formed, underlain by peat deposits with a thickness of up to 2 m. A more detailed description of stratigraphy and stratigraphic section is available in previous studies [35, 42, 44].

2.2. Sample Collection and Analytical Methods

During the summer season, sediment samples were collected from the dump, peat deposits along the stream, and rock deposits from a borehole located near the dump (**Figure 1**). Peat samples were taken from pits at depths of 0–0.6 m using disposable polyethylene bags. Rock sediments were obtained during borehole flushing. Each sample weighed approximately 500 g. The collected samples were air-dried, ground using a vibratory mill, and sieved. Quartering was performed to ensure representative subsampling for all samples.

X-ray diffraction (XRD) was conducted on fractions ground to a grain size of 1–2 mm. Samples were further

pulverized in an agate mortar with alcohol and applied onto glass slides. Samples were analyzed in triplicate. Analyses were conducted in triplicate using a DRON-8 automated powder diffractometer (Innovation Center "Burevestnik", Russia) with CuKα radiation and a Mythen 2R1D multichannel detector. Diffraction patterns were scanned over a 2θ range of 3°–65° with a step size of 0.1°, and the dwell time at each point was 5 s. The primary beam slit width was 0.5 mm, and the samples were rotated at a speed of 1 rpm. The relative error of peak intensity measurement was 5% for mass fractions >10% and 10% for mass fractions <10%.

The bulk elemental composition of the sediments was analyzed using X-ray fluorescence (XRF) with synchrotron radiation and detection via an Si(Li) detector at the Siberian Synchrotron and Terahertz Radiation Center (INP SB RAS). For quality control, the IAEA/SOIL-7 standard (Laboratory Seibersdorf, Vienna, Austria) was included with each batch of digestion. Instrumental uncertainties were below 10%.

The composition, size, and quantitative distribution of mineral phases were studied using a MIRA 3 LMU scanning electron microscope (Tescan Ltd) equipped with an INCA Energy 450 XMax 80 microanalysis system (Oxford Instruments Ltd – NanoAnalysis Ltd). This system utilized thermionic field emission. Imaging conditions included secondary electron (SE) and backscattered electron (BSE) modes, an accelerating voltage of 20 kV, a beam current of 1.6 nA, and an acquisition time of 10 s per analysis. Microinclusions in minerals smaller than 20 μm were identified considering the composition of surrounding minerals. Detection limits for most elements ranged between 0.2–0.3 wt.%. For trace elements, acquisition times were extended to 150 s to improve detection limits.

2.3. Experimental Procedure

The experimental determination of uranium forms in sediments was conducted using a modified selective fractionation method based on the Tessier procedure[45].

The following sequential extraction procedure was employed:

1. Water soluble uranium: Extraction with distilled water (H_2O, V = 25 ml, T = 25°C, t = 1 h);
2. Exchangeable uranium: Extraction with 1M NH_4OAc solution (pH 7, V = 25 ml, T = 25 °C, t = 1 h);
3. Uranium bound to carbonates Extraction with 1M NH_4OAc buffered with HOAc (pH 5, V = 25 ml, T = 25 °C, t = 5 h);
4. Uranium bound to humic acids: Extraction with 0.01M NaOH solution (pH 11, V=25 ml, T = 25 °C, t = 12 h);
5. Uranium bound to oxides: Extraction with 2M $NH_2OH{\cdot}HCl$ in 25% HOAc (pH 2, V = 25 ml, T = 96 °C, t = 6 h);
6. Uranium bound to organic matter: Extraction with 30% H_2O_2 containing 0.02M HNO_3 (pH 2, V = 20 ml, T = 85 °C, t = 24 h);
7. Residual uranium: Acid decomposition using a mixture of HF-HNO_3-$HClO_4$-HCl.

At the end of each extraction step, the residue was washed with 10 ml of distilled water and centrifuged at 4500 rpm. The initial sample weight for each experiment was 2 g.

The resulting solutions from each stage were transferred into 15 ml tubes for subsequent analysis of chemical composition. Elemental determinations, excluding uranium, were carried out using an inductively coupled plasma optical emission spectrometer (ICP-AES) Agilent 5100 (Agilent Technologies, Australia). Uranium concentrations were analyzed using an inductively coupled plasma mass spectrometer (ICP-MS) NexION 300D (PerkinElmer, USA). The relative error of these methods did not exceed 3%.

3. Results and Discussion

3.1. Chemical Composition and Properties of Sediments

The results of the chemical analysis of the sediments are presented in **Table 1**. In the sediments of the dump, uranium concentrations exceed background levels by three orders of magnitude, reaching 200 g t^{-1}. In the peat deposits of the stream behind the dam, the uranium concentration decreases sharply to 40 g t^{-1}. However, further downstream in the peat deposits of the swamp, uranium concentrations increase significantly, reaching 730 g t^{-1}.

Such variation can primarily be attributed to the high content of organic matter in peat deposits: due to the substantial inflow of water masses and reduced streamflow velocity, the floodplain becomes increasingly waterlogged. Humic acid, the primary component of peat organic matter, plays a significant role in binding trace elements through chelation

on its surface[46]. Additionally, under these conditions, the number of microorganisms consuming nitrate ions increases, thereby reducing and precipitating uranium[35, 36]. The high organic matter content in peat deposits also promotes uranium sorption processes, immobilizing it[44].

Table 1. Bulk elemental composition of sediments.

Elements		Peat Sediments				Rock Sediments
		Dump	Stream	Swamp	Stream Fork	
As	ppm	1968	992	3097	1144	29
Ba		934	633	1076	1050	561
Co		210	900	252	291	28
Cr		58	161	103	65	132
Cu		162	183	515	217	41
Li		81	237	248	54	111
Mo		259	55	395	417	1.2
Ni		327	350	521	615	77
Pb		219	42	714	247	27
Sr		267	4.7	168	209	262
U		206	42	730	79	0.5
V		80	235	158	86	181
W		223	216	305	78	2.3
Zn		263	697	437	313	114
Al	%	2.9	2.9	10.7	4.1	3.6
Ca		6.8	6.8	4.9	1.5	2.0
Fe		3.5	3.5	7.2	3.7	3.5
K		0.7	0.7	3.1	1.1	1.1
Mg		0.3	0.3	2.0	0.4	0.5
Mn		4.2	4.2	1.8	3.7	7.9
Na		0.9	0.9	1.2	0.7	0.6
P		0.2	0.2	0.2	0.2	0.2
Ti		0.1	0.1	0.5	0.2	0.2
S		0.4	0.4	0.2	0.4	0.2

The increased uranium concentration in peat deposits highlights the role of reducing conditions in immobilizing uranium, favoring its stabilization in tetravalent forms. These forms are significantly less mobile than their hexavalent counterparts, commonly found under oxidizing conditions[30, 35, 36]. This geochemical behavior underscores the critical influence of organic matter and associated microbial activity in controlling uranium mobility and distribution.

In peat deposits collected from the stream fork, the uranium concentration is 80 g t^{-1}. With increasing distance from the facility, the concentration decreases, reaching 5.5 g t^{-1} in pond sediments, which still exceeds background levels — according to Taylor[47], the Clarke concentration of uranium is 2.5 g t^{-1}.

Despite the proximity to the contamination source, uranium concentrations in rock sediments are 0.5 g t^{-1}.

In addition to uranium, elevated levels were observed for heavy metals, particularly arsenic and lead, as well as lithium and zinc: their concentrations in samples from the dump were 1970, 220, 81, and 263 g t^{-1}, respectively, exceeding background levels by orders of magnitude — the Clarke concentrations of arsenic are approximately 7 g t^{-1}, lead 10 g t^{-1}, lithium 20 g t^{-1}, and zinc 70 g t^{-1} [47]. The high concentrations of these metals are linked to industrial processes: metallic lithium and its compounds are produced at NCCP; zinc is used in uranium ore processing; manganese serves as a reducing agent in the technology; while arsenic and lead are impurities associated with uranium mineralization[43]. These elevated concentrations of heavy metals, alongside uranium, suggest potential synergetic effects on mobility and environmental risks.

X-ray diffraction analysis revealed a high organic matter content in the peat — over 50% of the total mass (**Table 2**). Additionally, manganese and iron oxides (hausmannite and hematite) were found at levels ranging from 5% to 20%. The deposits also include calcite, micaceous minerals, and quartz. Silicates, feldspars (including plagioclase), and amphiboles are present in subordinate amounts.

In rock sediments, the mineral composition corresponds to that of sands, sandy loams, and loams of the Quaternary sediments: a significant amount of quartz was identified, with lesser amounts of plagioclase, potassium feldspar, and mica. Amphibole and calcite were identified as minor minerals.

3.2. Uranium Speciation in Sediments Based on Selective Fractionation Experiments

The results of selective fractionation experiments revealed that the majority of uranium in the sediments transitions into poorly soluble forms (**Figure 2**).

In the rock sediments, nearly 80% of uranium is present in its most stable form associated with silicates (residual uranium), 15% is found in the oxidizable form (uranium bound to organic matter), and 5% is associated with iron and manganese oxides. X-ray diffraction analysis did not reveal any discrete uranium mineral phases. Thus, all uranium in the rock sediments is isomorphically incorporated into accessory minerals.

In peat sediments, uranium is primarily characteristically associated with manganese and iron oxides. In the stream fork and swamp deposits, 55% of uranium is bound to iron and manganese, in the stream deposits — 45%, and in the dump deposits — 35%. Approximately 40% of ura-

Table 2. Mineralogical composition of sediments based on XRD analysis.

Sample		Mineralogical Composition
Peat sediments	Dump	>50% of X-ray amorphous phase (organic matter); 3–5% of calcite, hematite (Fe_2O_3), hausmannite (Mn_3O_4), mica; 2–3% of quartz, chalcopyrite; 1% of plagioclase
	Stream	20–25% of X-ray amorphous phase (organic matter); 20–25% of mica; 10–15% of chlorite, chlorite/smectite, quartz; 2–3% of plagioclase, calcite, chalcopyrite; 1% of amphibole and potassium feldspar
	Swamp	>50% of X-ray amorphous phase (organic matter); 10–15% hausmannite (Mn_3O_4); 10–15% of hematite (Fe_2O_3); 3–5% of mica, quartz, anhydrite; 2–3% of chlorite/smectite, plagioclase; 1% of amphibole
	Stream fork	>50% of X-ray amorphous phase (organic matter); 10–15% hausmannite (Mn_3O_4); 3–5% of mica, chlorite/smectite, quartz; 2–3% of feldspars, amphibole
Rock sediments		20–25% of quartz; 20–25% of chlorite/smectite; 10–15% of mica and chlorite; 3–5% of plagioclase; 2–3% of potassium feldspar and calcite; 1% of amphibole

nium in the dump deposits is associated with organic matter, 20–25% in the stream and swamp deposits, and about 5% in the stream fork deposits. This distribution can be attributed to the binding properties of humic acids, which, as a significant component of organic matter, retain uranium through active functional groups [46]. Between 10% and 20% of uranium in the peat is associated with the carbonate fraction, and a similar proportion is bound to silicates. Only 5% of uranium is observed in the water-soluble form. These findings confirm that organic matter and metal oxides are critical in limiting uranium mobility under reducing conditions. The high proportion of uranium bound to oxides and organic matter reflects its affinity for stable geochemical phases in such environments, reducing the risk of migration. These mechanisms highlight the importance of hydrogeochemical conditions in designing effective containment strategies for radionuclide storage systems [30, 37].

Analysis of the sediments using scanning electron microscopy (SEM) confirmed the presence of the following minerals: a large amount of iron and manganese oxides, barite, and apatite; to a lesser extent, quartz, plagioclase, alkali feldspar, and pyrite (chalcopyrite occurs in minor amounts), as well as chlorite and fluorite. Rutile is occasionally observed (**Figure 3a**), which is associated with the low migration capacity of titanium under exogenous conditions, leading to its accumulation in waterlogged areas. In one instance, a silver-selenium compound identified as naumannite (**Figure 3b**) (a disilver selenide with iron impurities) was detected, as well as phosphosilicate (**Figure 4a**).

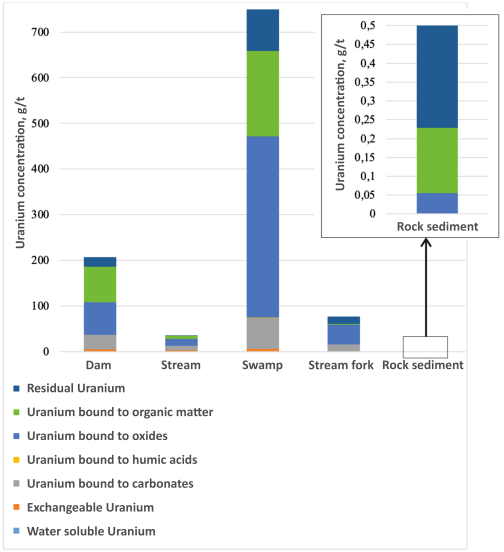

Figure 2. Uranium speciation in sediments.

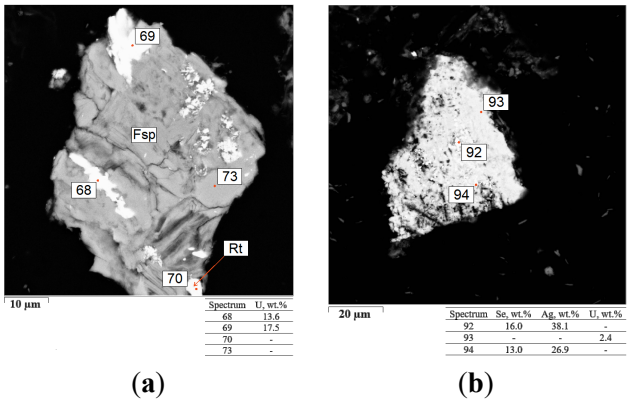

(a) **(b)**

Figure 3. SEM images: (**a**) feldspar grain (Fsp) with rutile (Rt); (**b**) naumannite.

Uranium is found in significant quantities with metal

oxides, more commonly with manganese than with iron. XRD analysis of the peat revealed a high content of manganese oxides (hausmannite) and iron oxides (hematite), comprising 5–15% of the total mass (**Table 2**). No discrete uranium mineral phases were detected. The formation of uranium mineral phases associated with metal oxides was confirmed using SEM (**Figures 4b** and **5a,b**). Since manganese concentrations in peat exceed those of iron (**Table 1**), uranium is primarily associated with hausmannite (**Figure 5a**). Manganese oxides form fine-grained inclusions, appearing as either individual fragments no larger than 10 μm or as loose, larger clusters resembling concretions, with sizes exceeding several hundred microns. The uranium content in these minerals varies between 0.5 and 10 wt%. The strong association of uranium with manganese oxides suggests that manganese plays a more dominant role than iron in uranium immobilization. This association aligns with previous studies indicating the high sorption capacity of manganese oxides for radionuclides under reducing conditions [37].

In smaller amounts, uranium associated with iron was detected in the sediment samples. Uranium phases were concentrated around the periphery of iron hydroxide grains, with uranium content reaching a few percent by weight (**Figure 6a**). Additionally, in the stream fork peat sample, a magnetite grain was observed with a rim containing uranium at a concentration of 0.4 wt% (**Figure 6b**). The cross-sectional size of the grain is 60 μm, and its surface is fractured, but organic relics can be traced.

In the swamp peat sample, plate-like crystals of uranyl phosphate with a tetragonal structure were observed, which were not found in other areas of the sludge storage facility. Similar mineral forms are described in Doynikova et al. [48], where tetragonal calcium phosphorus silicate was identified in the Dalmatovskoe deposit, Russia, with the formula $(U^{4+},Ca,Fe)[(Si,P)(O,OH)_4]$. The size of individual crystals ranges from 5 to 40 μm, with uranium concentrations reaching 66 wt%.

All samples showed a high content of organic matter, ranging from 20% to over 50%. More detailed examination of the peat samples using EDS mapping for uranium revealed high uranium concentrations (**Figure 7a,b**). Uranium was evenly distributed over the surface of the peat particles, suggesting sorption by the peat's organic matter. The uranium content varied from 7 to 38 wt%.

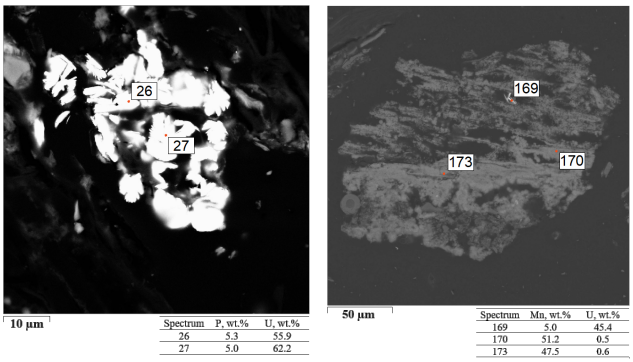

(**a**) (**b**)

Figure 4. SEM images of uranium mineral phases: (**a**) with phosphosilicate; (**b**) with manganese oxides.

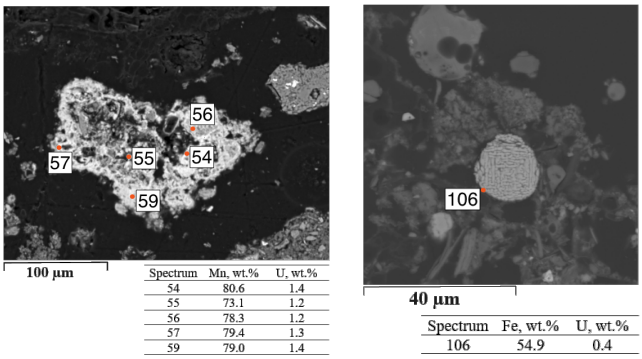

(**a**) (**b**)

Figure 5. SEM images: (**a**) hausmannite containing uranium; (**b**) hematite grain containing uranium.

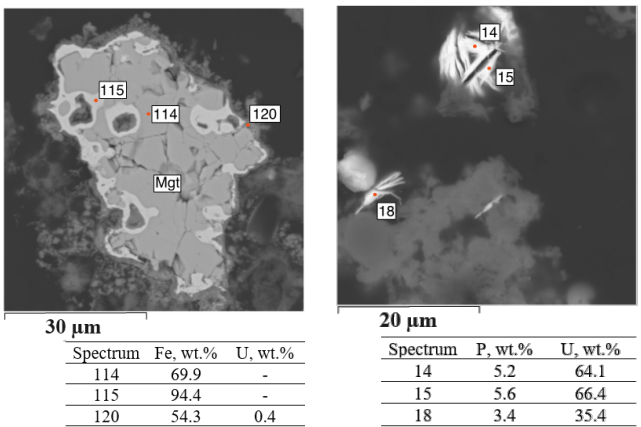

(**a**) (**b**)

Figure 6. SEM images: (**a**) magnetite grain with uranium (Mgt—magnetite); (**b**) coffinite.

4. Conclusions

The conducted study identified the main forms of uranium occurrence in the sediments of the sludge storage fa-

cility of Novosibirsk Chemical Concentrates Plant and the adjacent areas. It was established that in rock sediments, uranium predominantly exists in a stable residual form associated with silicates, whereas in peat deposits, up to 55% of uranium is associated with iron and manganese oxides, and up to 40% is bound to organic matter. The most mobile forms of uranium (water-soluble and exchangeable) account for less than 5% of the total content.

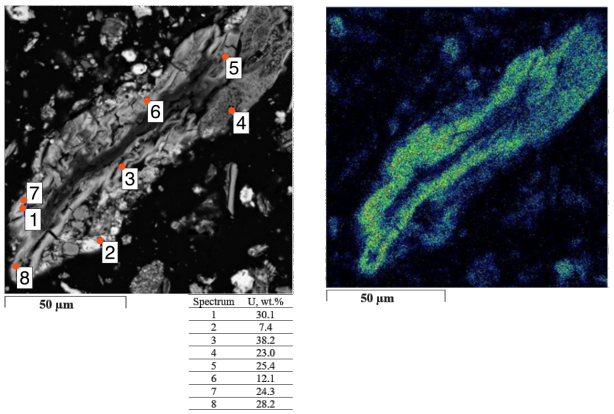

Spectrum	U, wt.%
1	30.1
2	7.4
3	38.2
4	23.0
5	25.4
6	12.1
7	24.3
8	28.2

(a) **(b)**

Figure 7. SEM images: (**a**) peat particle with uranium; (**b**) EDS mapping of the peat particle for uranium.

The results showed that uranium concentration significantly decreases with distance from the tailings repository, primarily due to sorption processes involving the organic matter in peat deposits and co-precipitation with mineral components. Manganese and iron oxides, as well as humic acids, play a pivotal role in limiting uranium migration, as confirmed by X-ray diffraction analysis and scanning microscopy data.

These findings highlight the necessity of considering the specific features of the geochemical environment when developing strategies for the environmentally safe management of sludge storage facilities. Natural sorbents, such as organic matter and metal oxides, can provide the foundation for effective natural barriers to limit radionuclide migration. These results are critical for assessing environmental risk and planning measures to minimize the negative impact of low-level radioactive waste on the environment.

Future research should account for various environmental conditions, such as changes in redox potential, the composition of surface and groundwater, including radionuclide migration forms, and the role of microbial processes in radionuclide transformation. These factors will provide a broader context for understanding radionuclide interactions in diverse geochemical systems. Such studies will enhance predictive models of radionuclide behavior, assess their potential for bioremediation strategies, and inform waste management practices at specific facilities.

Author Contributions

Conceptualization, O.S.; methodology, O.S.; formal analysis, D.M.; investigation, O.S. and D.M.; writing—original draft preparation, O.S.; visualization, D.M.; supervision, O.S.; funding acquisition, O.S. All authors have read and agreed to the published version of the manuscript.

Funding

This work was supported by the Russian Science Foundation grant number 23-27-00362, https://rscf.ru/en/project/23-27-00362/.

Institutional Review Board Statement

Not applicable.

Informed Consent Statement

Not applicable.

Data Availability Statement

Data will be available on request from the corresponding author.

Acknowledgment

The authors thank Boguslavsky A.E., the head of the Laboratory for Modeling the Dynamics of Endogenous and Technogenic Systems of the V.S. Sobolev Institute of Geology and Mineralogy Siberian Branch Russian Academy of Science, for providing materials for this work and the scheme of the sludge storage site.

Conflicts of Interest

The authors declare no conflict of interest.

References

[1] Letuvinkas, A.I., 2002. Anthropogenic geochemical anomalies and the natural environment. NTL: Tomsk, Russia. pp. 1–92. (in Russian).

[2] Choppin, G.R., 2007. Actinide speciation in the environment. Journal of Radioanalytical and Nuclear Chemistry. 273, 695–703. DOI: https://doi.org/10.1007/s10967-007-0933-3

[3] Runde, W.H., 2000. The chemical interactions of actinides in the environment. Los Alamos Science. 26, 392–411

[4] Senko, J.M., Jonathan, D.I., Joseph, M.S., et al., 2002. In-situ evidence for uranium immobilization and remobilization. Environmental Science & Technology. 36(7), 1491–1496. DOI: https://doi.org/10.1021/es011240x

[5] Novikov, A.P., Vlasova, I.E., Safonov, A.V., et al., 2018. Speciation of actinides in groundwater samples collected near deep nuclear waste repositories. Journal of Environmental Radioactivity. 192, 334–341. DOI: https://doi.org/10.1016/j.jenvrad.2018.07.007

[6] Novikov, A.P., 2010. Migration and concentration of artificial radionuclides in environmental objects. Geochemistry International. 48, 1263–1387. DOI: https://doi.org/10.1134/S001670291013001X

[7] Istok, J.D., Senko, J.M., Krumholz, L.R., et al., 2004. Environmental Science & Technology. 38(2), 468–475. DOI: https://doi.org/10.1021/es034639p

[8] Romanchuk, A.Yu., Vlasova, I.E., Kalmykov, S.N., 2020. Speciation of uranium and plutonium from nuclear legacy sites to the environment: A mini review. Frontiers in Chemistry. 11(3), 61–65. DOI: https://doi.org/10.3389/fchem.2020.00630

[9] Majumder, E.L.-W., Wall, J.D., 2017. Uranium biotransformations: Chemical or biological processes. Open Journal of Inorganic Chemistry. 7, 28–60. DOI: https://doi.org/10.4236/ojic.2017.72003

[10] Ure, A.M., Davidson, C.M., 2007. Chemical speciation in the environment, 2nd ed. Blackwell Science: Glasgow, Scotland. 1–452. DOI: https://doi.org/10.1002/9780470988312

[11] Newsome, L., Morris, K., Lloyd, J.R., 2014. The biogeochemistry and bioremediation of uranium and other priority radionuclides. Chemical Geology. 363, 164–184. DOI: https://doi.org/10.1016/j.chemgeo.2013.10.034

[12] Buddemeier, R.W., 1988. Transport of colloidal contaminants in groundwater: Radionuclide migration at the Nevada test site. Applied Geochemistry. 3, 535–548.

[13] Kersting, A.B., Efurd, D.V., Finnegan, D.L., et al., 1999. Migration of plutonium in ground water at the Nevada Test Site. Nature. 397(6714), 56–59

[14] McCarthy, J.F., 1989. Subsurface transport of contaminants. Environmental Science & Technology Journal. 23, 496–502

[15] Vilks, P., 1991. Sorption behaviour of 85Sr, 131I and 137Cs on colloids and suspended particles from the Grimsel test site, Switzerland. Applied Geochemistry. 6, 553–563

[16] Weisbrod, N., Dahan, O., Adar, E.M., 2002. Particle transport in unsaturated fractured chalk under arid conditions. Journal of Contaminant Hydrology. 56(2), 117–136. DOI: https://doi.org/10.1016/s0169-7722(01)00199-1

[17] Kalmykov, S., Zakharova, E., Novikov, A., et al., 2011. Effect of redox conditions on actinide speciation and partitioning with colloidal matter. In: Kalmykov, S., Denecke, M. (eds.). Actinide Nanoparticle Research. Springer: Berlin/Heidelberg, Germany. pp. 361–375. DOI: https://doi.org/10.1007/978-3-642-11432-8_13

[18] Wu, W.M., Carley, J., Luo, J., et al., 2007. In situ bioreduction of uranium (VI) to submicromolar levels and reoxidation by dissolved oxygen. Environmental Science & Technology Journal. 41(16), 5716–5723. DOI: https://doi.org/10.1021/es062657b

[19] Ilina, S.M., Marang, L., Lourino-Cabana, B., et al., 2020. Solid/liquid ratios of trace elements and radionuclides during a nuclear power plant liquid discharge in the Seine River: Field measurements vs geochemical modeling. Journal of Environmental Radioactivity. 32560877, 220–221. DOI: https://doi.org/10.1016/j.jenvrad.2020.106317

[20] Shotyk, W., Bicalho, B., Cuss, C.W., et al., 2017. Trace metals in the dissolved fraction (<0.45μm) of the lower Athabasca River: Analytical challenges and environmental implications. Science of the Total Environment. 580, 660–669. DOI: https://doi.org/10.1016/j.scitotenv.2016.12.012

[21] Cuss, C.W., Grant-Weaver, I., Shotyk, W., 2017. AF4-ICPMS with the 300 da membrane to resolve metal-bearing "colloids" < 1kDa: Optimization, fractogram deconvolution, and advanced quality control. Analytical chemistry. 89(15), 8027–8035. DOI: https://doi.org/10.1021/acs.analchem.7b01427

[22] Di Bonito, M., Lofts, S., Groenenberg, J.E., 2018. Models of geochemical speciation: Structure and applications. In: De Vivo, B., Belkin, H.E., Lima, A. (eds.). Environmental Geochemistry: Site Characterization, Data Analysis and Case Histories, 2nd ed. Elsevier: Amsterdam, Netherlands. pp. 237–305. DOI: https://doi.org/10.1016/B978-0-444-63763-5.00012-4

[23] Krawczyk-Bärsch, E., Scheinost, A.C., Rossberg, A., et al., 2020. Uranium and neptunium retention mechanisms in Gallionella ferruginea/ferrihydrite systems for remediation purposes. Environmental Science and Pollution Research. 28, 18342–18353. DOI: https://doi.org/10.1007/s11356-020-09563-w

[24] Safonov, A.V., Perepelov, A.V., Babich, T.L., et al., 2020. Structure and gene cluster of the O-

polysaccharide from Pseudomonas veronii A-6-5 and its uranium bonding. International Journal of Biological Macromolecules. 165, 2197–2204. DOI: https://doi.org/10.1016/j.ijbiomac.2020.10.038

[25] Rzhevskaia, A.V., Romanchuk, A.Y., Vlasova, I.E., et al., 2021. Partitioning of uranium in contaminated bottom sediments: The meaning of fractionation. Journal of Environmental Radioactivity. 1, 229–230. DOI: https://doi.org/10.1016/j.jenvrad.2021.106539

[26] Alekhin, Y.V., Ivleva, E.A., Il'ina, S.M., et al., 2020. Experimental fundamentals of the colloid hydrogeochemistry of continental runoff. Geochemistry International. 58(9), 1050–1060. DOI: https://doi.org/10.1134/S0016702920080030

[27] Winstanley, E.H., Morris, K., Abrahamsen-Mills, L.G., et al., 2019. U(VI) sorption during ferrihydrite formation: Underpinning radioactive effluent treatment. Journal of Hazardous Materials. 366, 98–104. DOI: https://doi.org/10.1016/j.jhazmat.2018.11.077

[28] Wiesmann, U., 1994. Biological nitrogen removal from wastewater. In: Ulber, R. (ed.). Biotechnics/Wastewater. Advances in Biochemical Engineering/Biotechnology. Springer: Berlin/Heidelberg, Germany. ABE(51), pp. 113–154.

[29] Toropov, A.S., 2020. Migration forms of anthropogenic radionuclides in tunnel waters at the Degelen mountains, Semipalatinsk test site. Geochemistry International. 58(3), 342–351. DOI: https://doi.org/10.1134/S0016702920020123

[30] Degueldre, C., Triay, I., Kim, J., et al., 2000. Groundwater colloid properties: A global approach. Applied Geochemistry. 15(7), 1043–1051. DOI: https://doi.org/10.1016/S0883-2927(99)00102-X

[31] De Jonge, M., Teuchies, J., Meire, P., et al., 2012. The impact of increased oxygen conditions on metal-contaminated sediments part I: Effects on redox status, sediment geochemistry and metal bioavailability. Water Research. 46(7), 2205–2214. DOI: https://doi.org/10.1016/j.watres.2012.01.052

[32] Malkovsky, V.I., Yudintsev, S.V., 2016. Model of colloidal transportation of radionuclides by groundwater. Doklady Earth Sciences. 470(1), 942–945. DOI: https://doi.org/10.1134/S1028334X16090051

[33] De Jonge, L.W, Moldrup, P., Rubæk, G.H., et al., 2004. Particle leaching and particle-facilitated transport of phosphorus at field scale. Vadose Zone Journal. 3(2), 462–470. DOI: https://doi.org/10.2136/vzj2004.0462

[34] Safonov, A., Lavrinovich, E., Emel'yanov, A., et al., 2022. Risk of colloidal and pseudo-colloidal transport of actinides in nitrate contaminated groundwater near a radioactive waste repository after bioremediation. Scientific Reports. 12(1), 15–21. DOI: https://doi.org/10.1038/s41598-022-08593-3

[35] Safonov, A.V., Boguslavskii, A.E., Boldyrev, K.A., et al., 2019. Biogenic factors of formation of geochemical uranium anomalies near the sludge storage of the Novosibirsk Chemical Concentrate Plant. Geochemistry International. 57, 709–715. DOI: https://doi.org/10.1134/S0016702919060090

[36] Boguslavsky, A., Shvartseva, O., Popova, N., et al., 2023. Biogeochemical in situ barriers in the aquifers near uranium sludge storages. Water. 15, 3020. DOI: https://doi.org/10.3390/w15173020

[37] Hilton, J., 1997. Aquatic radioecology post Chernobyl - a review of the past and a look to the future. Studies in Environmental Science. 68, 47–74

[38] Kumblad, L., Kautsky, U., Næslund, B., 2006. Transport and fate of radionuclides in aquatic environments – the use of ecosystem modelling for exposure assessments of nuclear facilities. Journal of Environmental Radioactivity. 87(1), 107–129. DOI: https://doi.org/10.1016/j.jenvrad.2005.11.001

[39] Choppin, G.R., Morgenstern A., 2001. Distribution and movement of environmental plutonium. Radioactivity in the Environment. 1, 91–105. DOI: https://doi.org/10.1016/S1569-4860(01)80009-7

[40] Hosseini, A., Thørring, H., Brown, J.E., et al., 2008. Transfer of radionuclides in aquatic ecosystems – default concentration ratios for aquatic biota in the Erica Tool. Journal of Environmental Radioactivity. 99(9), 1408–1429. DOI: https://doi.org/10.1016/j.jenvrad.2008.01.012

[41] Safonov, A.V., Boguslavsky, A.E., Boldyrev, K.A., et al., 2021. Geochemical modeling of the uranium behavior in groundwater near the sludge storages during bioremediation. Geochemistry International. 59(1), 56–65. DOI: https://doi.org/10.1134/S0016702921010080

[42] Boguslavsky, A.E., Gaskova, O.L., Naymushina, O.S., et al., 2020. Environmental monitoring of low-level radioactive waste disposal in electrochemical plant facilities in Zelenogorsk, Russia. Applied Geochemistry. 119, 104598. DOI: https://doi.org/10.1016/j.apgeochem.2020.104598

[43] Gaskova, O.L., Boguslavskii, A.E., Sirotenko, T.G., 2011. Geochemical composition of natural waters near a storage site of low-activity radioactive wastes. Water Resources. 38, 597–607. DOI: https://doi.org/10.1134/S0097807811050071

[44] Safonov, A.V., Boguslavsky, A.E., Gaskova, O.L., et al., 2021. Biogeochemical modelling of uranium immobilization and aquifer remediation strategies near NCCP sludge storage facilities. Applied Sciences. 11, 2875. DOI: https://doi.org/10.3390/app11062875

[45] Tessier, A., 1979. Sequential extraction procedure for the speciation of particulate trace metals. Analytical Chemistry. 51(7), 844–851.

[46] Odah, M.M., Naser, K.M., 2024. Effect of Humic acid and levels of Zinc and Boron on Chemical Behavior of Zinc in Calcareous Soil. Journal of Envi-

ronmental & Earth Sciences. 6(3), 143–155. DOI: https://doi.org/10.30564/jees.v6i3.7126

[47] Taylor, S.R., 1964. Abundance of chemical elements in the continental crust: A new table. Geochimica et Cosmochimica Acta. 28(8), 1273–1285.

[48] Doynikova, O.A., Sidorenko, G.A., Mokhov, A.V., et al., 2015. New data on phosphosilicates of tetravalent uranium. New Data on Minerals. 50, 11–19. (in Russian).